# Modelling study on freezing process of water droplet on inclined cold plate surface with droplet dynamic behavior considered

# Modelling study on freezing process of water droplet on inclined cold plate surface with droplet dynamic behavior considered

**Qun Dang[a], Mengjie Song[a,*], Xuan Zhang[a], Libor Pekař[b,d], Seyyed Hossein Hosseini[c]**

[a]*Department of Energy and Power Engineering, School of Mechanical Engineering, Beijing Institute of Technology, Beijing 100081, China*

[b]*Department of Automation and Control Engineering, Faculty of Applied Informatics, Tomas Bata University in Zlín, Nad Stránimi 4511, Zlín 76005, Czech Republic*

[c]*Department of Chemical Engineering, Ilam University, Ilam 69315-516, Iran*

[d]*Department of Technical Studies, College of Polytechnics Jihlava, Tolstého 16, 586 01 Jihlava, Czech Republic*

[*]*Corresponding author. E-mail address: mengjie.song@gmail.com (M. Song).*

**Abstract**

Droplet freezing on inclined surfaces exists widely in engineering fields. To accurately predict and control the freezing process of a sessile water droplet on inclined surface, a theoretical model based on the heat-enthalpy method is presented in this study, with two types of dynamic behavior considered, deformation and spreading. After the validation of model by droplet profiles and freezing duration from experiments, the freezing characteristics are analyzed, including contact area, frozen height and vertex offset, etc. As found, the effect of inclined angle on less than 10.34 $\mu$L water droplet is greater than that on larger than 10.34 $\mu$L droplet, due to the mutual relation between surface tension and gravity effect. When the inclined angle of surface changes from 0 ° to 40°, the contact area keeps at 11.61 mm$^2$ for 10 $\mu$L water droplet, and increases by 5.64% from 23.04 to 24.34 mm$^2$ for 25 pL water droplet. The initial heights of 10 and 25 pL water droplets decrease by 0.85% from 1.18 mm to 1.17 mm and by 1.91% from 1.51 mm to 1.49 mm, respectively. That means it is easier frozen for the same water droplet on bigger inclined angle surface. This study is beneficial for the optimization of anti-frosting and defrosting technologies.

**Keywords**: Sessile water droplet, inclined surface, dynamic behavior, freezing proces, modeling study

## 1. Introduction

Frosting and icing are common phenomena and have significant influences on industrial applications [**1,2**]. Frost and ice often pose hazards to a variety of applications, such as a heat pump [**3**] and aircraft [**4,5**]. For example, frost formed on the surface of a vaporizer would reduce the operation efficiency of air source heat pump [**6**]. The impacting and icing of a water droplet on the surfaces of an aircraft or cables may result in safety problems [**7**]. The freezing process of water droplet is at the start stage of frosting and icing, and thus influences the final formation of frost or ice [**8**]. To solve the frosting and icing problems, accurately predicting and controlling the freezing process of water droplet under various conditions are important.

According to temperature transition characteristics inside a droplet, the freezing process could be divided into four stages, including supercooling, recalescence, freezing and cooling stages [**9,10**]. The

studies about freezing characteristics at different stages have been widely investigated, such as nucleation characteristics [**11**], freezing front [**12**] and frozen tip [**13**], etc. For example, the nucleation characteristics have been investigated experimentally by Zhang et al. [**14**]. As reported, the nucleation rate increased with decrease of surface temperature and increase of droplet volume. For morphology of freezing front, it was experimentally investigated by Marin et al. [**15**] based on Hele-Shaw cell. Results indicated that the angles between of freezing front and solid-air boundary were about 87°. As for frozen tip of water droplet, the effect of gas concentration on it was experimentally investigated by Li et al. [**16**]. As reported, frozen tip angles are approximately $129.5° \pm 4.1°$ for water droplet with 3% gas concentration and $80.3° \pm 9.1°$ for sparkling water with 14.66% gas concentration. However, the studies listed above are all about freezing process of water droplet on horizontal surface, while most surfaces in industrial applications are inclined. And freezing process of water droplet on horizontal and inclined surfaces has obvious differences. When horizontal surface is tilted, the contact area and height of water droplet would be changed due to gravity effect and thus freezing characteristics, such as freezing rate and frozen height, are influenced. Therefore, investigating the freezing process of water droplet on inclined surface is necessary.

As for water droplet on inclined surface, there are some studies on the dynamic freezing process [**17,18**]. For example, the factors of frozen morphologies of water droplets impacting on a subcooled inclined surface were investigated by Zhu et al. [**19**]. Four types of frozen droplet morphologies, namely elliptical cap, half ring + cap I, half ring + cap II , and half ring + single ring, were reported. Investigation of the effect of inclined angle on droplet shape was performed by Jin et al. [**20**]. It was found that at lower inclined angles, such as 0°, 30°, or 45°, the inclined angle of the surface had an apparent influence on the final shape of the ice bead. The above studies are mainly about freezing process of impacting water droplet. However, when a water droplet is condensed and frozen on a cold tilted surface, the state of water droplet during whole process is sessile. As for the freezing process of sessile water droplet on the inclined surface, there are some studies about frozen tip. For example, the frozen tip shifting increased as the increase of difference between front and rear contact angles [**21**]. In addition, the effect of heat flux direction on the orientation of frozen tip on inclined surface was also experimentally investigated by Starostin et al. [**22**]. But the effects of volume and inclined angle on freezing characteristics, such as contact area and frozen height, were not quantitatively investigated. Meanwhile, with more uncertainty factors resulting from experimental methods, theoretical models can provide an alternative approach to investigate the freezing process of water droplet. Thus, it is necessary to numerically investigate the freezing process of sessile water droplet on the inclined surface.

To better understand the freezing mechanisms, some efforts have been made to numerically investigate the freezing process of water droplets with different solution methods, such as heat-enthalpy method [**23**], lattice Boltzmann method [**24**] and fronttracking method [**25**]. For freezing process of water droplet on horizontal surface, a theoretical model based on heat-enthalpy method was developed by Lu et al. [**26**], with an average deviation of 0.17% for freezing time. The deviation was caused by assumption that the heat conduction at freezing front was one-dimensional and the thermal conductivity was stable. A model based on lattice Boltzmann method was developed by Sun et al. [**27**], of which average deviations for surface temperature cases of -29.5 °C, -15.6 °C and -9.5 °C are 2.87%, 3.00% and 2.50%, respectively. However, these models for horizontal surface are not applicable to the freezing process of sessile water droplet on inclined surface. The difficulty of modeling the freezing process of water droplet on inclined surface would be increased by the shape asymmetry and droplet dynamic behavior caused by gravity effect.

**Nomenclature**

| Variable | description Unit |
|---|---|
| $b$ | half width of droplet m |
| $Bo$ | bond number / |
| $c$ | specific heat kJ/(kg·°C) |
| $g$ | gravitational acceleration m/s$^2$ |
| $\vec{g}$ | gravity vector / |
| $h$ | droplet height m |
| $H$ | freezing front height m |
| $k$ | thermal conductivity W/(m·°C) |
| $L$ | latent heat of freezing kJ/kg |
| $P_0$ | pressure at the origin Pa |
| $P_{liq}$ | pressure of liquid atmosphere Pa |
| $P_{Ftm}$ | pressure of atmosphere Pa |
| $\Delta P_F$ | pressure difference from $P_0$ caused by the gravity Pa |
| $r$ | distance from the origin m |
| $r_F$ | front radius m |
| $r_R$ | rear radius m |
| $\vec{r}$ | distance vector from the origin / |
| $R$ | radius of spherical cap m |
| $R_0$ | contact radius of droplet on horizontal surface m |
| $R_{1,2}$ | principal radius of curvature on the liquid-gas interface m |
| $R_m$ | mean curvature m$^{-1}$ |
| $t$ | time s |
| $T$ | temperature °C |
| $\Delta T$ | supercooling degree °C |
| $v$ | freezing rate m/s |
| $V$ | actual volume of droplet m$^3$ |
| $V_c$ | calculated volume of droplet m$^3$ |
| $x$ | radius coordinate m |
| $\Delta x$ | gravity center offset m |
| $y$ | width coordinate m |
| $z$ | height coordinate m |

*Greek symbols*

| | |
|---|---|
| $\alpha$ | inclined angle rad |
| $\beta$ | ratio of major to minor axis of the ellipse / |
| $\rho$ | density of droplet kg/m$^3$ |
| $\varphi$ | angular parameter from x-axis rad |
| $\gamma$ | solid-gas surface tension mN/m |
| $\theta$ | contact angle rad |
| $\theta_D$ | dynamic growth angle rad |
| $\psi$ | tip angle rad |

*Superscripts*

| | |
|---|---|
| * | nondimensional / |

*Subscripts*

| | |
|---|---|
| c | critical / |
| F | front / |
| i | ice / |
| m | mixture / |
| N | nucleation / |
| R | rear / |
| w | water / |
| 0 | initial / |

Thus, there are few relevant studies. For example, freezing process of water droplet on inclined surface was simulated with a front-tracking method by Vu et al. [**28**], with assumption of unchanged contact line between water droplet and inclined surface during surface tilting process. Thus, this model is not applicable when droplet dynamic behavior during surface tilting process has a strong effect on freezing process. In addition, there are many freezing characteristics, including contact area, frozen height and frozen tip, etc. But previous studies mainly considered a few characteristics. For example, a "two-triangle" model with shape asymmetry of droplet considered is proposed to simulate frozen tip by Ismail and Waghmare [**21**], with deviations of $\pm$ 8 ° for tip angle, while other freezing characteristics

are not investigated. Therefore, a theoretical model on freezing process of water droplet on inclined cold surface with dynamic behavior during tilting process and freezing characteristics fully considered is necessary.

Above all, most numerical studies are about the freezing process of sessile water droplet on horizontal surfaces [**29,30**], while surfaces inclined are not especially considered. Freezing characteristics of water droplet on inclined surface are not fully reported, and the dynamic behavior of water droplet during tilting process of surface was always ignored. In this study, a new theoretical model is presented to study the freezing process of water droplet on inclined surface, with two types of dynamic behavior, deformation and spreading, especially considered. After the model is validated experimentally, the effects of inclined angle and droplet volume on freezing characteristics, such as contact area, frozen height and frozen tip, are investigated. These fundamental data are not only meaningful to predict the freezing process of water droplet, but also make contributions to control freezing process and thus control the later icing and frosting process.

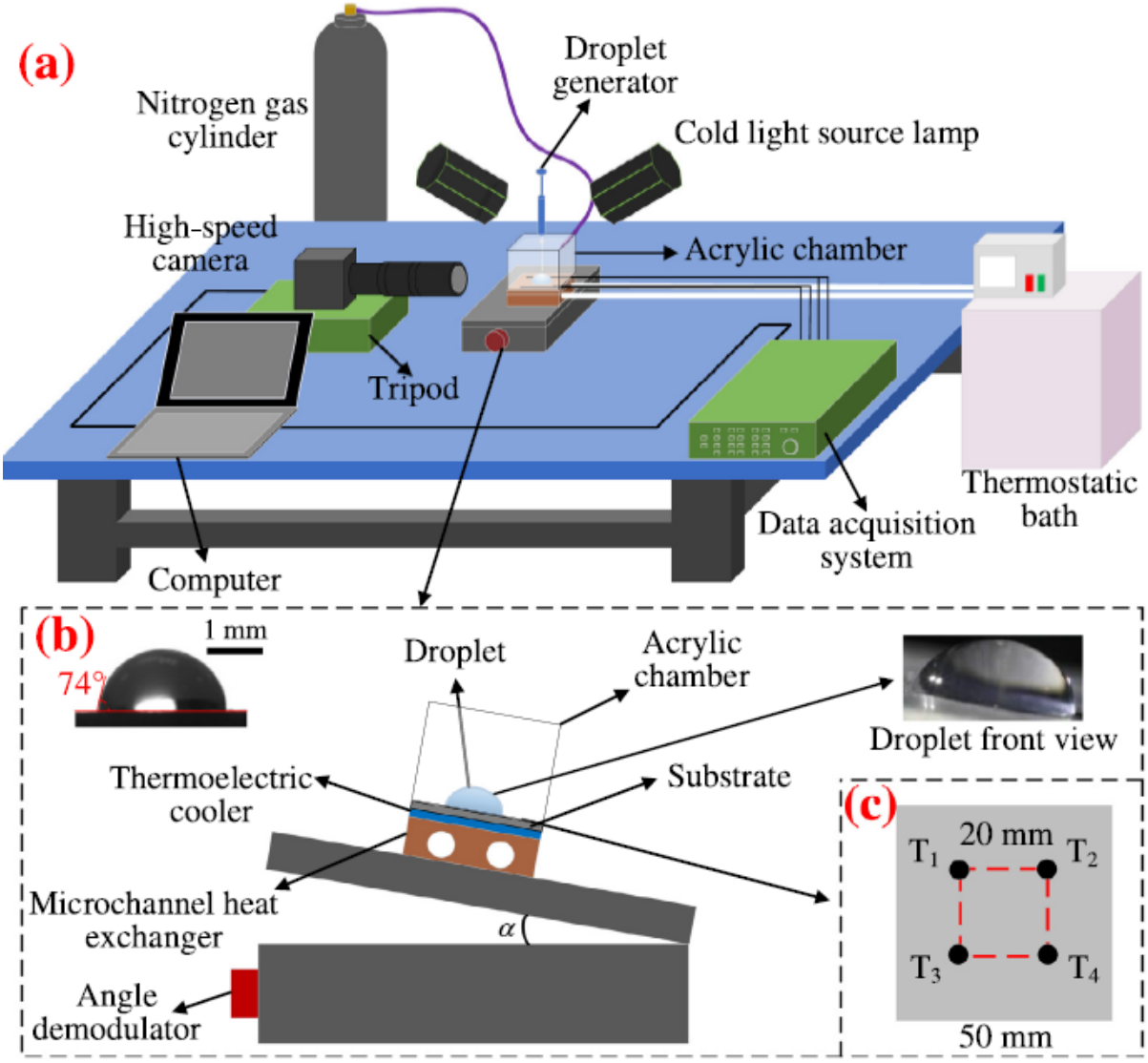


**Fig. 1**. Schematic diagram of experimental system.

**Table 1** Advancing and receding angles for surface used in this study.

| Droplet volume (μL) | Advancing angle (°) | Receding angle (°) |
|---|---|---|
| 15 | 87.64 | 63.46 |
| 20 | 91.54 | 62.88 |
| 25 | 91.43 | 61.60 |
| 30 | 96.21 | 57.24 |

## 2. Methodology

### *2.1. Experimental work*

To observe and compare the freezing processes of water droplets on surface with various tilt angles, an experimental system setup is shown in **Fig. 1**(a). The whole experimental system includes four parts, a test section, a semiconductor thermoelectric cooling system, a data acquisition system and environmental protection section. In the test section, the water droplets generated from a pipette are solidified on the surface of the cold plate at dimensions of 40 x 40 $mm^2$ . The precision accuracy of pipette with a range of 5 $\sim$ 20 $\mu$L is $\pm$ 0.1 $\mu$L. On the surface of plate with a roughness of 3.2 $\pm$ 0.2 Ra, water droplet static contact angle is measured at 74° $\pm$ 0.3°, as shown in **Fig. 1**(b). The advancing and receding angles of different water droplets on this surface are shown in Table 1. The average advancing and receding angles are 92.53 ° and 60.47°, respectively. To prevent frosting on the surfaces, a cubic acrylic chamber with side length of 40 mm is made and filled with nitrogen gas. For semiconductor thermoelectric cooling system used to control the surface temperature, it includes a 72 W thermoelectric chilling plate with dimensions of 40 x 40 x 6.4 $mm^3$ , a direct current power supplier with reference voltage of 12 V, a thermostatic bath with minimum temperature of -50 °C and a microchannel heat exchanger at dimensions of 40 x 40 x 20 $mm^3$ . To minimize the temperature decreasing duration, temperature of working medium in thermostatic bath, glycol aqueous solution, is always fixed at -40 °C.

The data acquisition system is divided into image and temperature acquisition systems. In the image acquisition system, highspeed camera is used to capture the freezing processes of water droplets. Two cold light source lamps are used outside the chamber, with soft light paper between lamps and chamber to disperse the light. In the temperature acquisition system, $K$-type thermocouples, with precision accuracy of $\pm$ 0.1 °C, are used. To measure cold plate surface temperature accurately, four thermocouples are placed at different places as a square shape, as shown in **Fig. 1**(c). The side length of the square is 20 mm, about 50% of the side length of the aluminum plate. The maximum temperature difference among the measurement data of four thermocouples, $T_1$, $T_2$, $T_3$ and $T_4$ , is less than 0.2 °C. To measure the temperature of nitrogen in the chamber, two thermocouples are placed at 20 mm and 40 mm above the surface, respectively. The above temperatures are monitored by a temperature data acquisition system with a frequency of 2 Hz or a data every 0.5 s.

The main concern of this study is about freezing process of sessile water droplet on the cold plate surface with tilt angles. Thus, the inclined angles a are set in the range of 0 $\sim$ 40°, with intervals of 10°. The Bond number of water droplet, with a volume of 10.34 $\mu$L, is 1. When the water droplet volume is larger than 10.34 $\mu$L, gravity effect on initial droplet profile should be considered. To balance the gravity effect on droplet profile, the droplet volumes $V_0$ are set in the range of 5 $\sim$ 20 $\mu$L, with intervals of 5 $\mu$L. To investigate the influence of surface temperature $T_s$ , the freezing processes of water droplets on horizontal surface with different temperature are observed. If the surface temperature is set at above -10 °C, the water droplet may be not frozen. Considering 5 cases of surface temperature

are necessary to show influence of surface temperature on the freezing process, the surface temperatures are set in the range of -30 —10 °C, with intervals of 5 °C. To study the freezing processes of water droplets on horizontal and inclined surfaces, 36 experimental cases are designed and listed in **Table 2**.

**Table 2** 36 experimental cases designed in this study.

| Case No. | Water | | | Case No. | Water | | |
|---|---|---|---|---|---|---|---|
| | $\alpha$ (°) | $T_s$ (°C) | $V_0$ (μL) | | $\alpha$ (°) | $T_s$ (°C) | $V_0$ (μL) |
| 1–4 | 0 | -30 | 5, 10, 15, 20 | 21–24 | 0 | -10 | 5, 10, 15, 20 |
| 5–8 | 10 | -30 | 5, 10, 15, 20 | 25–28 | 0 | -15 | 5, 10, 15, 20 |
| 9–12 | 20 | -30 | 5, 10, 15, 20 | 29–32 | 0 | -20 | 5, 10, 15, 20 |
| 13–16 | 30 | -30 | 5, 10, 15, 20 | 33–36 | 0 | -25 | 5, 10, 15, 20 |
| 17–20 | 40 | -30 | 5, 10, 15, 20 | | | | |

*2.2. Description of theoretical model*

To numerically investigate the freezing process of water droplets on inclined surface, a theoretical model is presented in this study. To simplify the model, the following seven assumptions are adopted in this model.

1. The freezing front is flat and parallel to the inclined surface;
2. The cold plate has uniform roughness and the droplet contact angle is fixed;
3. The heat conduction is one-dimensional and the thermal conductivity is stable;
4. The nucleation locations of droplets are at three-phase line and time is fixed;
5. The ice crystals during recalescence stage are distributed uniformly in droplet;
6. Heat transfer and evaporation between droplet and surrounding air are neglected;
7. Clear ice is generated that means no air bubble is trapped in frozen water droplet.

*2.2.1. Dynamic behavior during initial stage*

A water droplet is placed on the horizontal surface and then the surface is tilted slowly, the droplet starts to be deformation. During this process, the dynamic behavior of the water droplet could be divided into two types, deformation and spreading. The front, side and top views of droplet under deformation type after static are described by **Fig. 2**(a1-c1), respectively. Under deformation type, the droplet profile would be deformation due to the gravity effect, as shown in **Fig. 2**(a1). Because the effect of surface tension on droplet profile is greater than gravity effect, the contact line between droplet and surface keeps circular, as shown in **Fig. 2**(c1). The mass center of droplet changes from point $O$ to $O_1$, and its offset is Ax. Those views of droplet under spreading type after static are shown in **Fig. 2**(a2-c2). Under spreading type, the balance between surface tenson and gravity is broken due to the increase of volume. The contact line starts to spread until reaching balance, as shown in **Fig. 2**(a2). The contact line changes from circular to a combined shape of a circular and an elliptical, as shown in **Fig. 2**(c2). The mass center of droplet changes from point $O$ to $O_2$ . The influences of gravity relative to surface tension on the droplet profile could be evaluated by Bond number, $Bo = pgR^2/y$. When $Bo > 1$, the influence of gravity is greater than that of surface tension and this means the water droplet is under spreading type. On the contrary, the droplet is under the deformation type. The

initial droplet profiles on the inclined surface under different types are mainly described by Young-Laplace equation and calculated by using different solutions.

*2.2.2. Droplet profile under deformation type*

Young-Laplace equation equates the Laplace pressure to the hydrostatic pressure,

$$P_{\mathrm{liq}} = P_{\mathrm{atm}} - 2\gamma H = P_0 + \rho \vec{g} \cdot \vec{r} \tag{1}$$

$$R_{\mathrm{m}} = \frac{1}{2}\left(\frac{1}{R_1} + \frac{1}{R_2}\right) \tag{2}$$

where, $P_{liq}$ , $P_{atm}$ are the pressures of liquid and atmosphere, respectively. $y$ and $p$ are the surface tension and density of liquid, respectively. $P_0$ is the pressure at the origin and $Rm$ is the mean curvature. And $R_1$, $R_2$ are the principal radii of curvature on the liquid-gas interface, which are in the plane perpendicular to the droplet surface.

On the three-dimensional spherical polar coordinates sketched in **Fig. 2**(a1), $\vec{g}$ = (gsin a, 0 . -gcos a)is the gravity vector. Then Eq. (1) can be rewritten as follows,

$$P_{\mathrm{atm}} - 2\gamma R_{\mathrm{m}} = P_0 - \rho g r \cos\alpha \cos\theta + \rho g r \sin\alpha \cos\theta \cos\varphi \tag{3}$$

where,$\alpha \in [0 . \pi]$ is the inclined angle of surface, and $\theta \in [0 . \theta_0]$ is the contact angle at different azimuth $\varphi \in [-\pi, \pi]$ . 00 is the initial contact angle on the horizontal surface. To simplify the calculation, Eq. (**3**) is converted to a dimensionless equation. And some parameters are defined as,

$$\begin{cases} r^* = r/R \\ R_{\mathrm{m}}^* = RR_{\mathrm{m}} \\ P^* = PR/\gamma \end{cases} \tag{4}$$

where, $R$ is the radius of spherical cap, as shown in **Fig. 2**(a1). Then Eq. (**3**) is rewritten as the one-dimensional Young-Laplace equation,

$$P_{\mathrm{atm}}^* - 2R_{\mathrm{m}}^* = P_0^* - Bo \times r^* \cos\alpha \cos\theta + Bo \times r^* \sin\alpha \sin\theta \cos\varphi \tag{5}$$

where, $Bo$ is the Bond number associated to the length $R$,

$$Bo = \frac{\rho g R^2}{\gamma} \tag{6}$$

When $Bo$ is less than 1, the droplet is so small that the gravity effect on the droplet can be neglected. An approximate solution to Eq. (**5**) may be obtained by a linear response argument. The deformation from the spherical cap is caused by gravity effect which is represented by two terms linear in $Bo$. As functions of azimuth $\varphi$, these terms generate a two-dimensional vector space, linear combinations

$c + dcos\varphi$ with $c, d$ functions of $\theta$. The linear response ansatz consists in looking for a solution to Eq. (**5**) in this vector space, at first order in $Bo$.

$$r^*(\theta, \alpha) = 1 + Bo \times r_{01}(\theta)\cos\alpha + Bo \times r_{11}(\theta)\sin\alpha\cos\varphi + O(Bo^2) \tag{7}$$

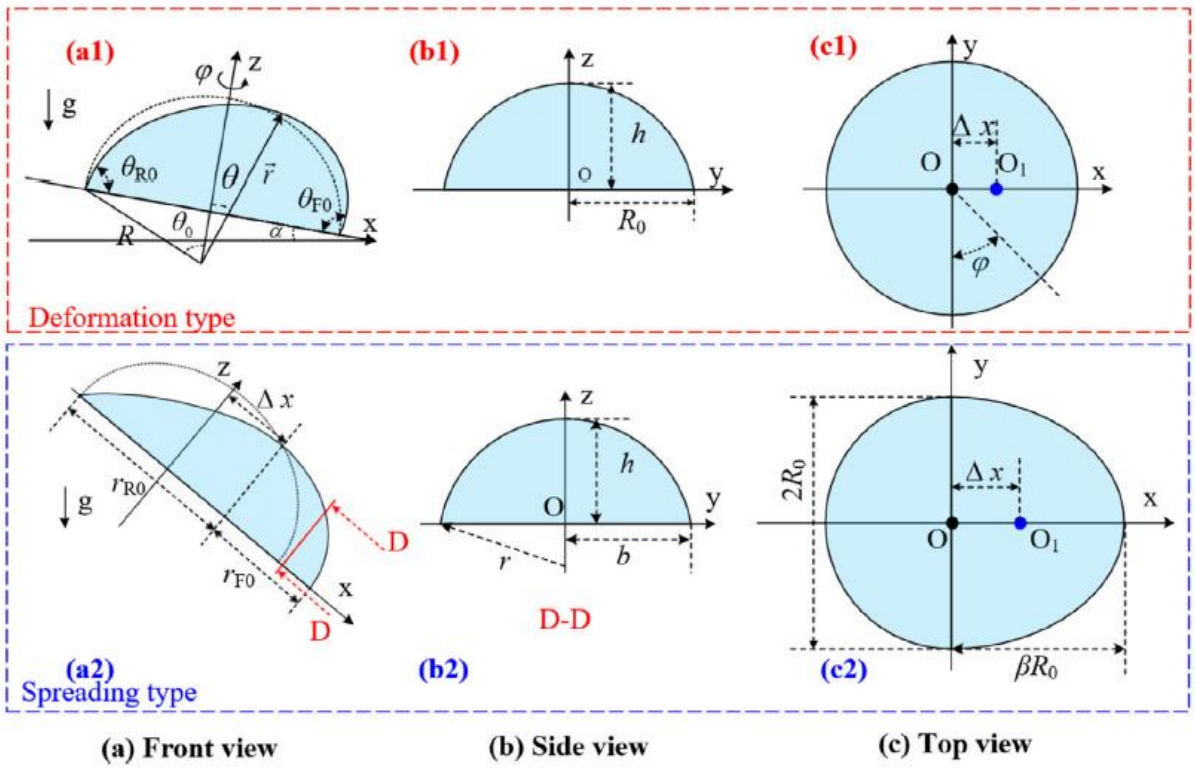


**Fig. 2**. Droplet profiles at the initial stage.

where, $r_{01}(\theta)$ and $r_n(\theta)$ are arbitrary functions of $\theta$, subject to the boundary conditions, and also subject to volume conservation at first order in Bo. They are expressed by Coninck et al. [**31**] as below,

$$\begin{cases} r_{01}(\theta) = \frac{\cos\theta - \cos\theta_0}{6} + \frac{\cos\theta}{3}\log\frac{1+\cos\theta_0}{1+\cos\theta} \\ r_{11}(\theta) = \frac{\sin\theta}{3}\left[\frac{\cos\theta}{1+\cos\theta} - \frac{\cos\theta_0}{1+\cos\theta_0} + \log\frac{1+\cos\theta}{1+\cos\theta_0}\right] \end{cases} \tag{8}$$

Then the linear response droplet profiles can be easily plotted by inserting Eq. (**8**) into Eq. (**7**). Two additional conditions are the boundary conditions for Eq. (**3**) as follows,

$$r(\theta_0, \varphi) = R \forall \alpha \tag{9}$$

$$V_c = \int_{\theta}^{\theta_0} \sin\theta d\theta \int_{-\pi}^{\pi} d\varphi \int_0^{r(\theta_0,\varphi)} r^2 dr \tag{10}$$

where, $V_c$ is the calculated volume of droplet. The initial droplet profile can be easily plotted by inserting Eq. (**8**) into Eq. (**9**) without $O(Bo^2)$. The convergence condition is when the calculated volume $V_c$ is equal to real volume of droplet.

*2.2.3. Droplet profile under spreading type*

The droplet profiles under spreading type are generally determined by the following three-dimensional Laplace equation [**32,33**],

$$\gamma \frac{-(1+z_y^2)z_{xx} + 2z_x z_y z_{xy} - (1+z_x^2)z_{yy}}{(1+z_x^2+z_y^2)^{3/2}} = P_0 + \Delta P_F \qquad (11)$$

The above equation indicates the force balance on the gas-liquid interface. In Eq. (**11**), $Zx$ etc. means the partial differentiation of $z = z(x, y)$ with respect to $x$. $P_0$ on the right hand side is the static pressure at the origin and is implicitly determined so as to satisfy the constraints, such as the droplet volume and the boundary conditions. $\Delta P_F$ indicates the difference of the pressure from P0 caused by the gravity.

To obtain the solution of Eq. (**11**) as simply as possible, the profile in the $yz$ cross section of droplet at each $x$ is approximated by a circle, as shown in **Fig. 2**(b2). The profile on the yz cross section can be written as,

$$\left(z + \frac{b^2 - h^2}{2h}\right)^2 + y^2 = \left(\frac{h^2 + b^2}{2h}\right)^2 \qquad (12)$$

$$x < 0 : b = \sqrt{R_0^2 - x^2} \qquad (13a)$$

$$x \geq 0 : b = \sqrt{R_0^2 - (x/\beta)^2} \qquad (13b)$$

where, $h = h(x)$ indicates the height of the droplet peak at $_D{-}D$ section. $b$ and $\beta$ are the half width of droplet at any $x$ and the ratio of major to minor axis of the ellipse, respectively. Since $z_y = 0$ at $z = h$ , Eq. (**11**) can be rewritten as follows at the peak line of droplet,

$$-\gamma \left[ \frac{z_{xx}}{(1+z_x^2)^{3/2}} + \frac{z_{yy}}{(1+z_x^2)^{1/2}} \right] = P_0 + \Delta P_F \qquad (14)$$

In Eq. (**14**), $z_{yy}$ can be calculated by Eqs. (**12**) and (13). Rewriting zxx and $z_y$ as $d^2 h/dx^2$ and $dh/dx$, the following ordinary differential equation for $h(x)$ is obtained after some arrangements as follows,

$$\gamma\left[-\frac{\frac{d^2h}{dx^2}}{\{1+(dh/dx)^2\}^{3/2}}+\frac{2h}{(h^2+b^2)\sqrt{1+(dh/dx)^2}}\right]=P_0-\Delta P_F \tag{15}$$

For droplet on the inclined surface, $\Delta P_F$ can be written as,

$$\Delta P_F=-\rho g\sin\alpha\cdot x-\rho gh\cos\alpha \tag{16}$$

Two boundary conditions are necessary to solve the second order ordinary differential Eq. (**15**). Two additional parameters, $\beta$ and $P_0$ , are needed to solve this equation. As a result, the following four conditions are considered.

$$x=-\beta a:\ h=0 \tag{17a}$$

$$x=-\beta a:\ \frac{dh}{dx}=\tan\theta_{F0} \tag{17b}$$

$$x=a:\ h=0 \tag{17c}$$

$$V_c=\int_{-R_0}^{\beta R_0}\left(\frac{h^2+b^2}{2h}\right)^2\left\{\cos^{-1}\left(\frac{b^2-h^2}{b^2+h^2}\right)-\frac{b^2-h^2}{b^2+h^2}\sqrt{1-\left(\frac{b^2-h^2}{b^2+h^2}\right)^2}\right\}dx \tag{17d}$$

where, $\theta_{F0}$ is the front angle. The volume of droplet can be calculated by Eq. (**17d**). The front and rear angles can be calculated by the following equations.

$$\cos\theta_{F0}=\cos\theta-\frac{\rho gV\sin\alpha}{4ka\gamma} \tag{18a}$$

$$\cos\theta_{F0}+\cos\theta_{R0}=2\cos\theta \tag{18b}$$

where, $k$ is the retentive-force factors, which is a constant $48/\pi^3$ [**34**]. For calculating simply, $\beta$ can be calculated by the empirical formula Eq. (**19**).

$$\beta=1+0.096\times Bo\times\sin\alpha \tag{19}$$

Inputting appropriate value of $P_0$ , the solution of Eq. (**15**) is obtained numerically by using the Runge-Kutta method [**35**] under the initial conditions of Eq. (**17a**) and (**17b**). $P_0$ is corrected repeatedly with Newton's method [**36**] to satisfy Eq. (**17c**) and (**17d**). Finally, the droplet profile under spreading type can be obtained.

*2.2.4. Droplet profile during recalescence stage*

During recalescence stage, the droplet changes into a uniform ice-water mixture due to supercooling effect. Its volume has a slight expansion because of the sudden change in density. Considering the supercooling effect on the physical properties of water droplet, the ice mass fraction, $\beta_i$ , can be determined by the energy balance as,

$$\beta_{\mathrm{i}} = \frac{c_{\mathrm{w}}(T_{\mathrm{F}} - T_{\mathrm{N}})}{L} \tag{20}$$

where, $T_N$ and $T_F$ are the nucleation and freezing temperatures, respectively. $c_w$ represents the water specific heat at $T_F$ , and $L$ represents the latent heat of water solidification. Then the latent heat, $L_m$ , and density, $\rho_m$ , of ice-water mixture can be calculated as follows:

$$L_{\mathrm{m}} = (1 - \beta_{\mathrm{i}})L \tag{21}$$

$$\rho_{\mathrm{m}} = (1 - \beta_{\mathrm{i}})\rho_{\mathrm{w}} + \rho_{\mathrm{i}}\beta_{\mathrm{i}} \tag{22}$$

where, $\rho_i$ and $\rho_w$ represent the densities of ice and water, respectively. When the surface temperature is -30 °C, the ice mass fraction of droplet at the end of recalescence stage is 0.38%. The volume expansion percentage due to slight change in density can be neglected. So, the droplet profile at the end of recalescence stage is similar to the profile at the initial stage.

*2.2.5. Droplet profile during freezing stage*

The freezing process of a sessile water droplet on an inclined cold plate is described by **Fig. 3**. To facilitate analysis and observation, the inclined coordinate system is changed to horizontal coordinate system, as shown in **Fig. 3**(a) and (b). During the following freezing stage, the ice-water mixture turns into absolutely ice. The region above the freezing front is ice-water mixture, and that below is solid ice. The mass conservation between them can be expressed as,

$$\rho_{\mathrm{m}}\frac{dV}{dt} = -\rho_{\mathrm{i}}\left[\frac{1}{2}\pi(r_{\mathrm{R}} - \Delta x)(r_{\mathrm{F}} + \Delta x) + \frac{1}{2}\pi(r_{\mathrm{R}} - \Delta x)^2\right]\frac{dH}{dt} \tag{23}$$

where, $V$ is the volume of ice-water mixture above freezing front, and $r_R$ and rF are rear and front radii, respectively, as shown in **Fig. 3**(c).

During freezing process, the ice-water mixture maintains constant at the freezing point temperature of 0 °C. The heat conduction on the freezing front is assumed to one-dimensional. The energy conversation at the freezing front can be described as,

$$\frac{k_{\mathrm{i}}\Delta T}{H} = \rho_{\mathrm{i}}L_{\mathrm{m}}\frac{dH}{dt} \tag{24}$$

where, $k$. represents the thermal conductivity of ice. By integrating Eq. (**24**), the relation between the height of freezing front, $H$, and freezing time, t, can be written as,

$$H = \sqrt{2\frac{k_{\mathrm{i}}\Delta T}{\rho_{\mathrm{i}}L_{\mathrm{m}}}t} \tag{25}$$

The height of unfrozen ice-water mixture above the freezing front can be calculated by,

$$h = \frac{\rho_{\mathrm{i}}}{\rho_{\mathrm{m}}}H \tag{26}$$

The relation between vertical freezing rate, $v$. and the height of freezing front can be written as,

$$v = \frac{dH}{dt} = \frac{k_{\mathrm{i}}\Delta T}{\rho_{\mathrm{i}}L_{\mathrm{m}}H} \tag{27}$$

As shown in **Fig. 3**(c), the rear and front horizontal freezing rates, $v_R$ and v $F$, can be expressed as,

$$\begin{aligned}\frac{dr_{\mathrm{R}}}{dt} &= v_{\mathrm{R}} = \frac{dH/dt}{\tan\theta_{\mathrm{R}}} = \frac{v}{\tan\theta_{\mathrm{R}}}\\ \frac{dr_{\mathrm{F}}}{dt} &= v_{\mathrm{F}} = \frac{dH/dt}{\tan\theta_{\mathrm{F}}} = \frac{v}{\tan\theta_{\mathrm{F}}}\end{aligned} \tag{28}$$

where, $\theta_R$ and $\theta_R$ represent the rear and front angles of ice-water mixture at three-phase line, respectively. At the start of freezing stage, the angles of $\theta_R$ and $\theta_F$ decrease as the height of three-phase line increases. But when 0R and 0F decrease to a certain angle, the contact angle starts to increase. The certain angle is called critical angle $\theta_c$, which is the main condition of frozen tip formation. Before reaching critical angle $\theta_c$, the angle between freezing direction of rear side and horizontal line is the same as the rear angle 0 R of ice-water mixture, when the angle at front side is the same as the front angle $\theta_F$ , as shown in **Fig. 4**(a). After reaching critical angle $\theta_c$, the Bond number of ice-water mixture is much less than 1. This means that the effect of gravity on ice-water mixture profile is much less than that of surface tension. The profile of ice-water mixture droplet tends to be spherical segment due to surface tension and thus its rear and front angles increase with the height of three-phase line. The angles between freezing directions and horizontal line are less than the rear angle $\theta_R$ and front angle $\theta_F$, as shown in **Fig. 4**(b). The difference is dynamic contact angle represented by $\theta_D$. Before critical angle, $r_R > r_F$ and $v_R > v_F$ . After reaching critical angle, $r_R = r_F$ and $v_R = v_F$. Therefore, rear and front angles when $\theta_R$ and $\theta_F$ are larger than $\theta_c$ can be expressed as,

$$\begin{cases}\theta_{\mathrm{R}} = ar\tan\frac{dh}{dr_{\mathrm{R}}}\\ \theta_{\mathrm{F}} = ar\tan\frac{dh}{dr_{\mathrm{F}}}\end{cases}\{\text{Before } \theta_{\mathrm{R,F}} = \theta_{\mathrm{c}}\} \tag{29}$$

where, $dh$ represents the height change of ice-water mixture at three-phase line. Critical angle $\theta_c$ is about $0.083\pi$, according to experimental data.

When $\theta_{\mathrm{R}}$ and $\theta_F$ decrease to $\theta_c$, $\theta_R$ and $\theta_F$ starts to increase with the height of three-phase line. Dynamic contact angle $\theta_D$ is changing with the height of three-phase line. To simplify the model, the relations of rear and front horizontal freezing rate, $v_R$ and $v_F$ , with vertical freezing rate v are empirical formula obtained from experimental data as,

$$\begin{cases} v_R = -2.45 + 3.14\frac{v}{v_c} \\ v_F = -2.44 + 3.09\frac{v}{v_c} \end{cases} \{\text{After } \theta_{R,F} = \theta_c,\ Bo < 1\} \quad (30)$$

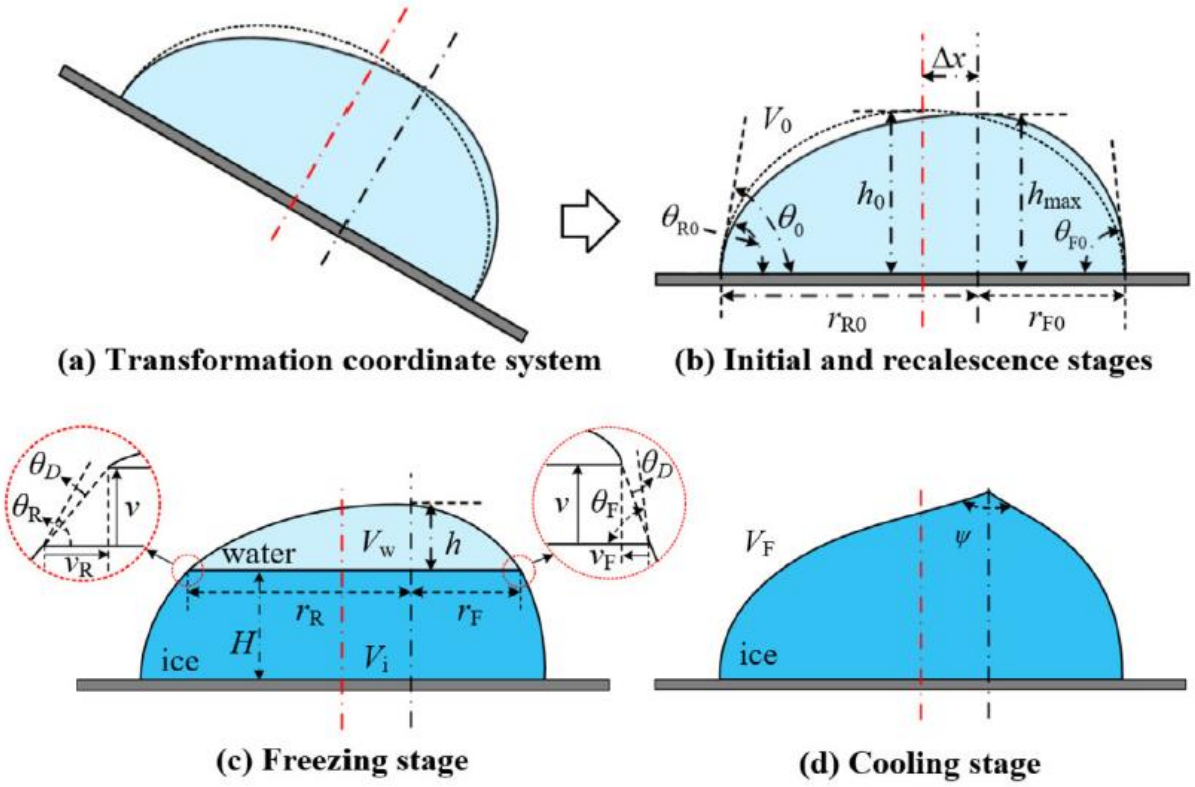


**Fig. 3**. Freezing process of a sessile water droplet on an inclined cold plate.

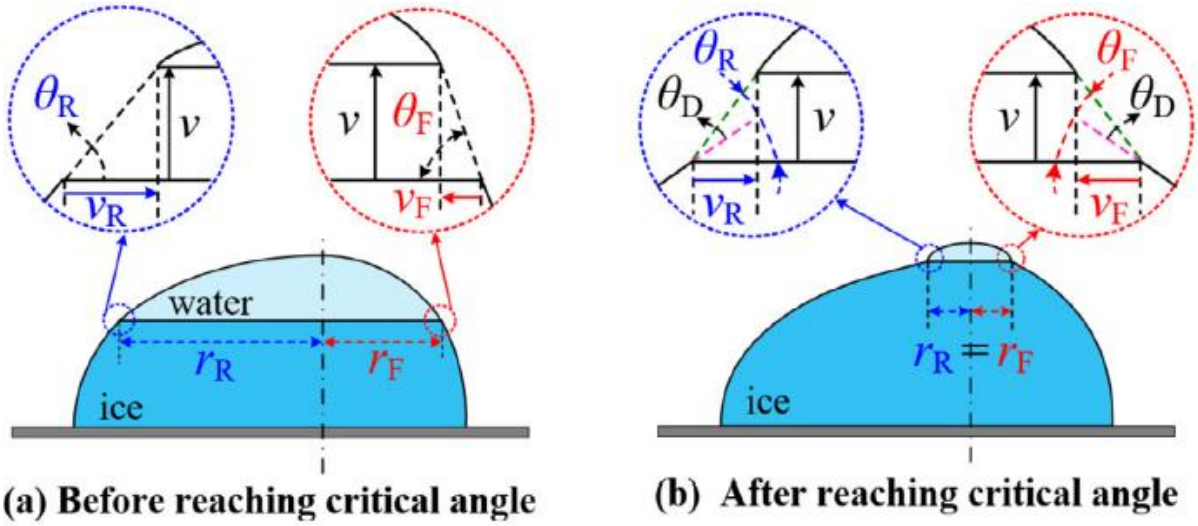


**Fig. 4**. Schematic diagram of critical angle at three-phase line during freezing process.

$$\begin{cases} v_{\mathrm{R}} = -2.07 + 2.53\frac{v}{v_c} \\ v_{\mathrm{F}} = -2.24 + 2.71\frac{v}{v_c} \end{cases} \{\text{After } \theta_{\mathrm{R,F}} = \theta_{\mathrm{c}}, Bo > 1\} \quad (31)$$

where, $v_c$ represents the vertical freezing rate when $\theta_R$ , $\theta_F = \theta_c$. $Bo$ ⟨ 1 represents that initial droplet profile is under deformation type, when Bo⟩ 1 represents the initial droplet profile is under spreading type.

According to Eqs. (**25**)—(**31**), the rear and front radii, $r_R$ and $r_F$ , can be expressed as,

$$\begin{cases} r_{\mathrm{R}} = r_{\mathrm{R0}} - \int_0^t v_{\mathrm{R}} dt \\ r_{\mathrm{F}} = r_{\mathrm{F0}} - \int_0^t v_{\mathrm{F}} dt \end{cases} \quad (32)$$

where, $r_{R0}$ and $r_{F0}$ represent the initial rear and front radii, as shown in **Fig. 3**(b). For droplets under deformation type, the profiles during freezing process can be calculated by Eqs. (**1**)—(**10**), (**23**)-(**30**) and (**32**). For droplets under spreading type, the profiles during freezing process can be calculated by Eqs. (**1**)—(**10**), (**23**)-(**29**) and (**31**), (**32**).

**Table 3** Physical properties of water and ice used in this study.

| Substances | $\rho_i$ (kg/m$^3$) | $c_w$ (kJ/(kg·K)) | $k$ (W/(m·K)) | $L$ (kJ/kg) |
|---|---|---|---|---|
| water | 1000 | 4.22 | 0.55 | 333.4 |
| ice | 917 | 2.05 | 2.16 | / |

*2.2.6. Calculation process of model*

The flowchart of calculating droplet profiles during freezing process is shown in **Fig. 5**. The physical properties of water and ice used in calculation process are shown in Table 3. With the known initial contact angle, volume and inclined angle, the calculation procedures can be described as follows. Different solutions of Young-Laplace equations from Refs. [**31-33**] are used to simulate the droplet profiles under different types at initial stage. At initial stage, calculate the Bo of the droplet firstly. If $Bo < 1$, the droplet profile is under deformation type. Young-Laplace equation is rewritten as one-dimensional equation [**31**]. The linear response ansatz is used to solve Eq. (**5**) in this vector space, at first order in $Bo$.

The calculated initial droplet profile is obtained by inserting Eq. (**8**) into Eq. (**7**). If the calculated results satisfy the convergence conditions Eqs. (**9**) and (**10**). The initial droplet profile under deformation type is obtained. For droplet of which $Bo > 1$ under spreading type, three dimensional Young-Laplace equation is rewritten as Eq. (**14**) which is the droplet profile under xz cross section [**32,33**]. The ratio of major to minor axis of the ellipse $\beta$ is calculated by empirical equation Eq. (**19**). And estimate an initial value of $P_0$. For example, $P_0$ is 60.09 Pa when a 20 $\mu$L water droplet is placed on a 40° inclined surface. Solving Eq. (**15**) with Rung-Kutta method under initial conditions of Eq. (**17a**) and **17b**) and $P_0$ is corrected repeatedly with Newton's method until satisfying Eq. (**17c**) and (**17d**). Then, the initial droplet profile under spreading type is obtained as the solution of Eq. (**15**) under the conditions of Eqs. (**17a**)-(**17d**). The droplet profile at initial stage can be calculated according to Eqs. (**1**)—(**10**) for deformation type and Eqs. (**11**)—(**19**) for spreading type. Then the profiles are outputted to the

recalescence stage. At recalescence stage, calculating the physical properties of ice-water mixture according to physical properties of water and ice. Then ouput the parameters to the freezing stage. At freezing stage, calculate $\theta_R$ and $0_F$ according to Eq. (**29**) firstly. Solve Eq. (**28**) before $\theta_R$ and $\theta_F$ reaching $\theta_c$. Then according Eqs. (**25**) and (**32**), the profiles during freezing stage can be calculated numerically. When the boundary conditions satisfy $r_R = r_F = 0$, frozen droplet profile is outputted.

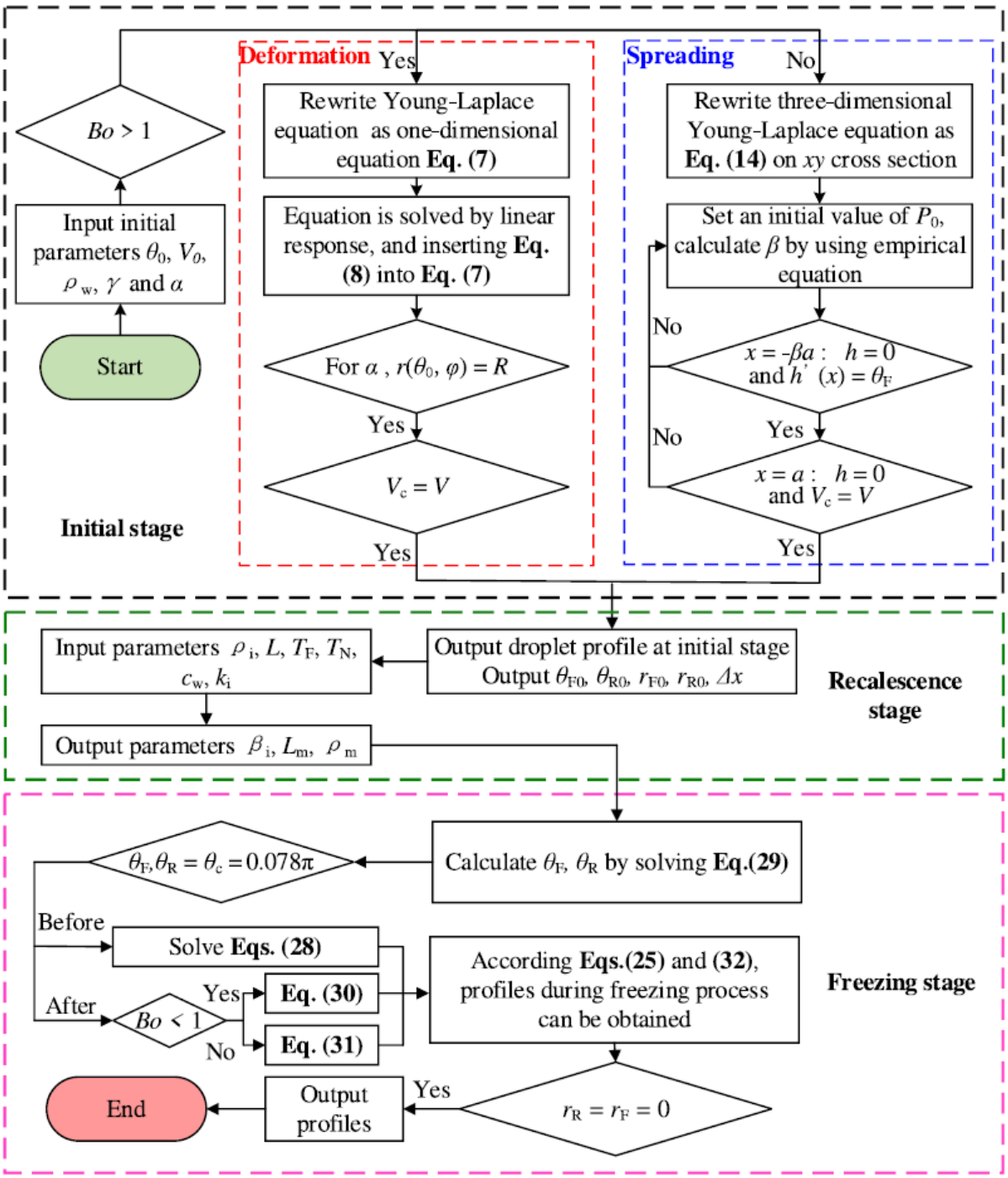


***Fig. 5**. Flowchart of calculating droplet profiles during freezing process.*

*2.3. Validation and evaluation of the model*

To validate this model, the simulation results and experimental data are compared. The freezing process of 5 and 20 $\mu$L water droplets on 40° inclined surface obtained from experiment and model are shown in **Figs. 6** and **7**, respectively.

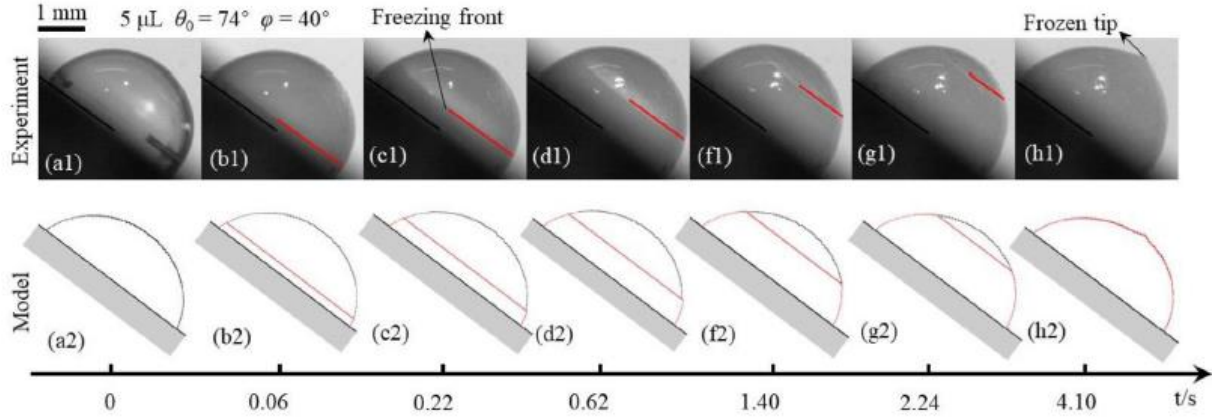


***Fig. 6****. Freezing process of a 5 μL water droplet on a 40° inclined surface obtained from experiment and model.*

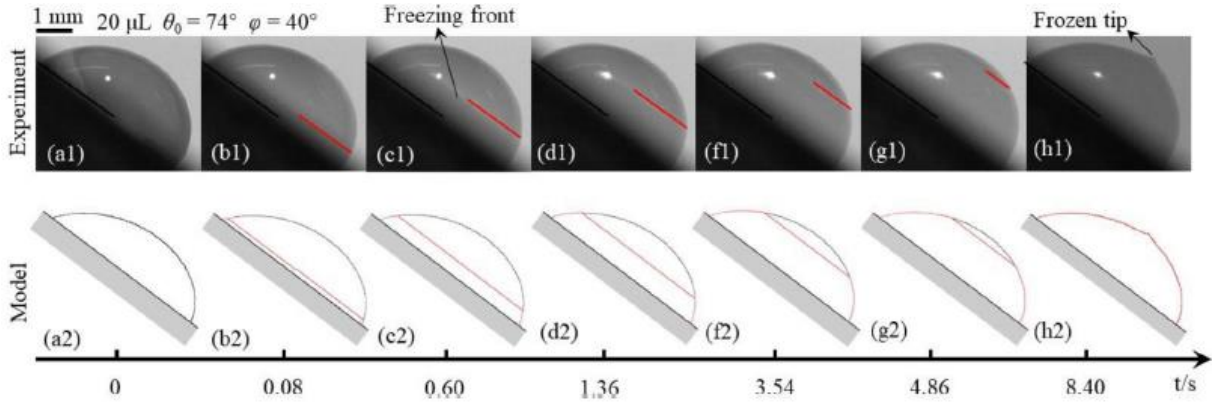


**Fig. 7**. Freezing process of a 20 $\mu$L water droplet on a 40° inclined surface obtained from experiment and model.

The experimental pictures are shown in **Figs. 6**(a1-h1) and **7**(a1-h1). And the simulation results are shown in **Figs. 6**(a2-h2) and **7**(a2-h2). The initial contact angle $\theta_0$ of water droplet on horizontal aluminum surface is 74° and the surface temperature is -30 °C. 5 and 20 $\mu$L water droplets on 40° inclined surface are under deformation and spreading types, respectively. As above mentioned, the whole freezing process could mainly be divided into four stages, initial, recalescence, freezing and cooling. Figs. 6(a1) and 7(a1) show the water droplet at the initial stage. Recalescence stage is between **Figs. 6**(a1),(b1) and **7**(a1),(b1). The recalescence durations are in the range of 24 ~ 48 ms. During freezing stage, freezing front is migrating up until the frozen tip formation. The freezing durations of 5 and 20 $\mu$L water droplets on 40° inclined surface with temperature -30 °C are 4.20 s and 8.18 s, respectively.

To make a more intuitive comparison between experiment and model, the initial and finial profiles obtained from **Figs. 6**(a1,a2,h1,h2) and **7**(a1,a2,h1,h2) are drawn at a coordinate system, as shown in **Fig. 8**(a). The data obtained from model agree well with the experimental data. The average deviations are all less than 6%. For 5 pL water droplet, the average deviations of initial and droplet profiles are 5.51% and 3.50%, respectively. And the maximum deviations are 13.76% and 16.54%, respectively. For 20 $\mu$L droplet, the average deviations of initial and droplet profiles are 4.09% and 4.27%, respectively. And the maximum deviation percentages are 12.17% and 17.07%, respectively. Actually, the maximum

deviation is less than 0.1 mm and the deviation percentage is 17.07% due to smaller denominator. The points of maximum deviations are all at the front side of droplet. The main reason may be the inaccurate calculation of front angle. Front angle is affected by many factors, physical properties of droplet, surface roughness and inclined angle, etc. For calculation of front angle, previous studies often used fitting experimental data to obtain empirical formulas [**34,37**]. For previous model of front angle, the deviations between calculated and experimental front angles were often in the range of 0° $\sim$ 20° [**38**]. In this study, the deviations of calculated front angles which are less than 10° can be acceptable.

To further validate model, the evolutions of freezing front height $H$, front and rear radii, $r_F$ and $r_R$ , obtained from experiment and model are compared in **Fig. 8**(b). During freezing stage, the height freezing front is increasing as time goes by, when front and rear radii are decreasing. Because the heat conduction during freezing process is assumed to be one-dimensional. When surface temperature is same, the evolutions of freezing front height for any water droplet are same according to Eq. (**25**). For 5 $\mu$L water droplet, the freezing duration obtained from experiment is 4.10 s while that calculated by the model is 4.22 s, the deviation is 2.90%. For 20 pL water droplet, the calculated freezing duration is 8.80 s when experimental duration is 8.40 s. The average deviation is 4.76%. The average deviations of freezing durations are all less than 5%, supporting the reliability of the model. A good agreement with experiment for freezing front $H$, rear radius $r_R$ , and front radius rF , obtained from model is observed. The average deviation of freezing front evolution is 2.27% and that of rear and front radii are 4.63 and 5.66%. As mentioned above, due to smaller denominator, the maximum deviations are 12.17% and 17.07%, respectively. The deviations are all less than 6%. This also supports the reliability of the model.

## 3. Results and discussion

The evolutions of front and rear angles with the height of three-phase line for 5 and 20 $\mu$L water droplet obtained from experiment are shown in **Fig. 9**. The initial contact angle $\theta_0$ of water droplet on the horizontal aluminum surface is 74°. As mentioned in **Section 2.2.5**, the whole freezing stage should be divided into two parts according to critical angle $\theta_c$. At the start of the freezing process, rear and front angles, $\theta_R$ and $\theta_F$, decrease as the height of three-phase line increases. When the angles decrease to critical angle, the rear and front angles, $\theta_R$ and $\theta_F$, start to increase until frozen tip formation. This phenomenon is caused by the evolution of gravity effect on water droplet. Freezing direction at three-phase line is tangential to the profile of water droplet at three-phase line. Before reaching critical angle, the gravity effect on water droplet profile is greater than surface tension. This means the angles between the droplet profile and horizontal line at three-phase line decrease as the height increases. But for after reaching critical angle, the effect of gravity on water profile is much less than that of surface tension. The profile of water droplet tends to be spherical segment due to surface tension and thus its contact angles between droplet and ice start to increase. As mentioned in our prior work, if rear and front angles consistently decrease with the height of three-phase line, the shape of frozen tip would be rounded instead of conical [**39**]. Therefore, critical angle is the main condition of conical frozen tip formation, as mentioned in **Section 2.2.5**. Critical angle is independent with droplet volume or inclined angle of surface. The critical angles are about 15° $\pm$ 2° for 5 $\mu$L and 15° $\pm$ 5° for 20 pL on surface with small tilt angles, as shown in **Fig. 9**.

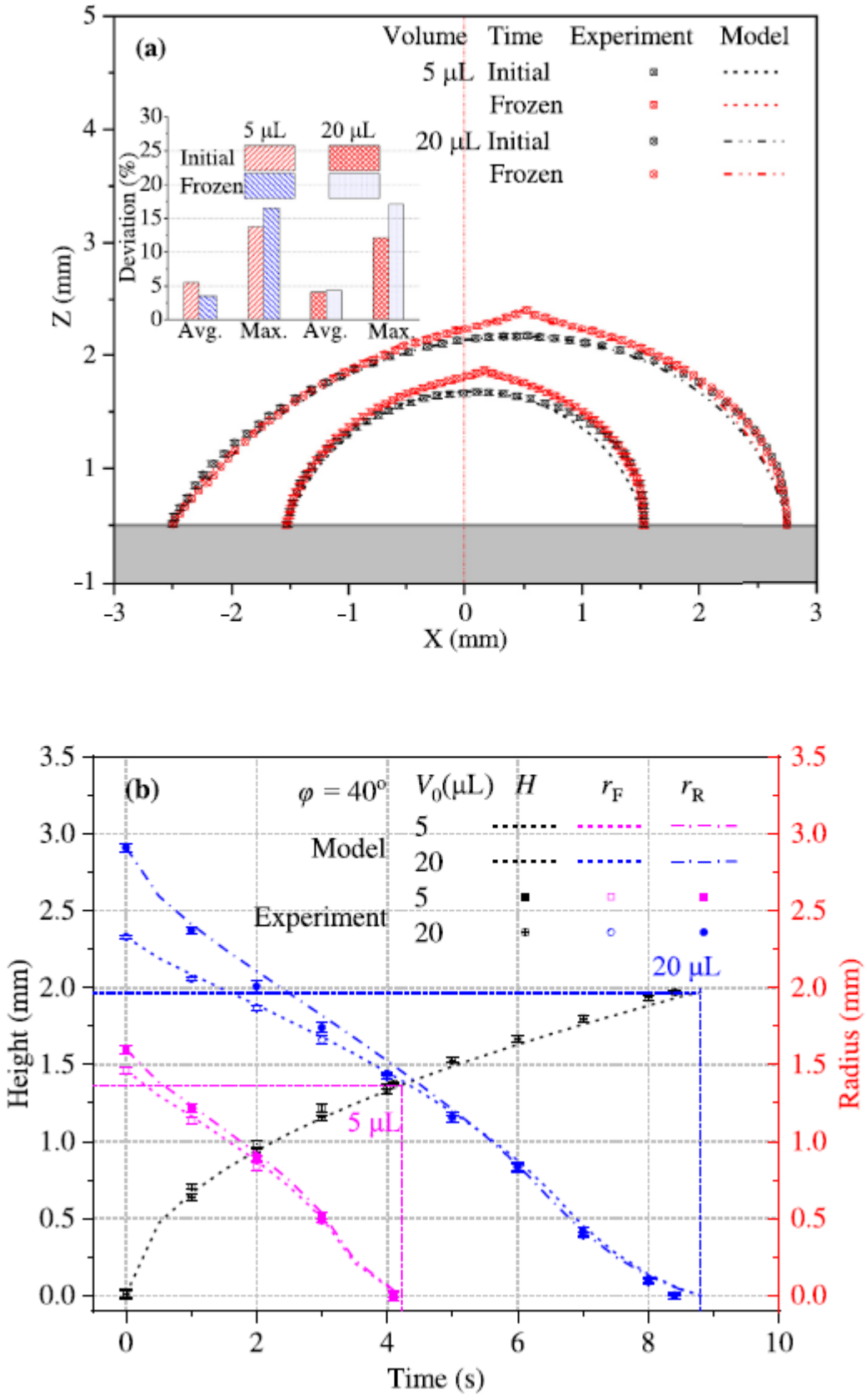


**Fig. 8**. Comparison of data obtained from experiment and model (a) initial and final profiles (b) freezing front height, front and rear radii.

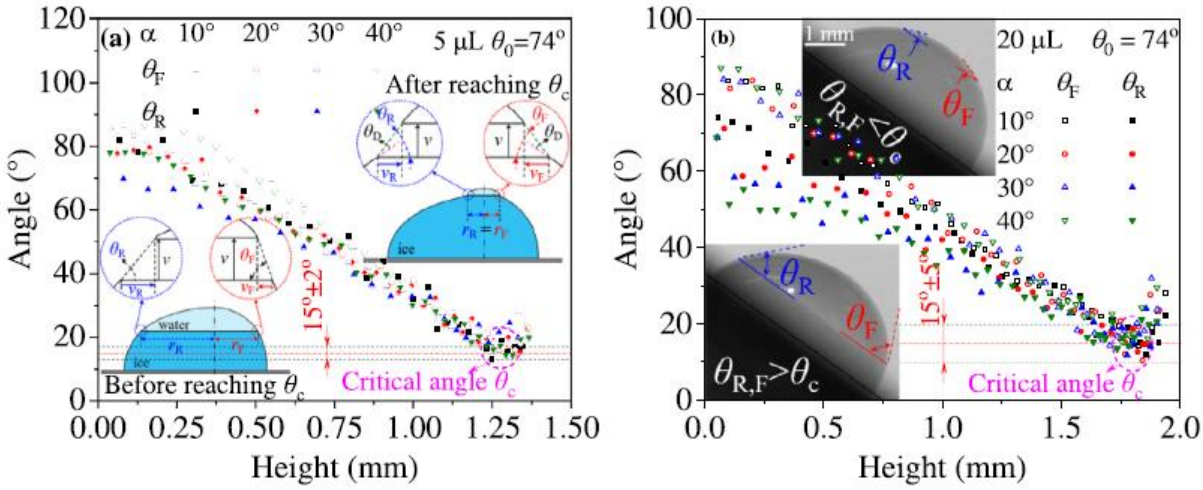


**Fig. 9**. Evolutions of front and rear angles with height (a) 5 |iL (b) 20 $\mu$L.

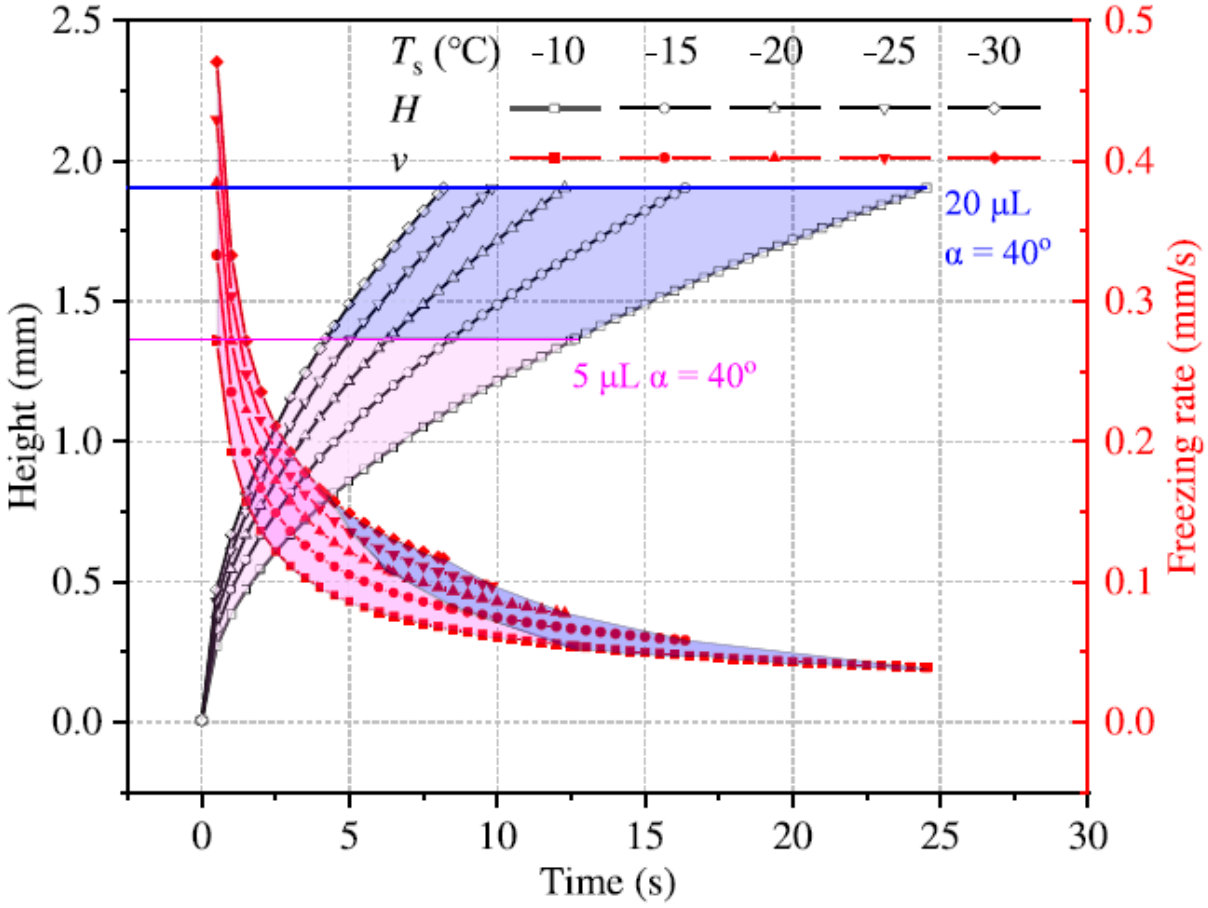


**Fig. 10**. Calculated evolution of freezing front height and freezing rate.

To predict the evolution of freezing front during freezing process and the effect of surface temperature on freezing process, the evolutions of freezing front height and freezing rate during freezing process are calculated. As an example, calculated data for 5 and 20 $\mu$L water droplet on 40° inclined surface with various surface temperatures are shown in **Fig. 10**. Because the heat conduction at freezing front is assumed to be one-dimensional. When the surface temperature Ts is same, the evolutions of freezing front heights H and freezing rates v for different volumes are same. The freezing durations are

different due to the different frozen heights. For example, when surface temperature Ts is -10 °C, the freezing front height of 5 $\mu$L water droplet increase to 1.37 mm at frozen time 12.64 s and that of 20 $\mu$L water droplet increase to 1.90 mm at frozen time 24.54 s. During freezing process, increase of ice thickness would increase thermal resistance, resulting in a decrease of freezing rate. When surface temperature Ts is -10 °C during freezing process, the freezing rate of 5 pL water droplet decreases by 62.96% from 0.27 to 0.10 mm/s and that of 20 $\mu$L water droplet decreases by 85.19% from 0.27 to 0.04 mm/s.

Changes of contact area and height would influence heat transfer rate and length, and thus influence freezing process. So, the effects of volume and inclined angle of surface on the droplet height and contact area are investigated, as shown in **Fig. 11**. For droplets under deformation type, the contact area does not change during the tilting process of surface due to the balance of surface tension and gravity. And the height has few changes. When the inclined angle of surface changes from 0° to 40° for 10 $\mu$L droplet, the contact area keeps at 11.61 mm$^2$ and the initial height decreases by 0.85% from 1.18 to 1.17 mm. The frozen height decreases by 0.76% from 1.32 to 1.31 mm. For droplets of which volume are larger than 10.34 $\mu$L, they are under spreading type. When the inclined angle of surface changes from 0° to 40° for 25 $\mu$L droplet, the contact area increases by 5.64% from 23.04 to 24.34 mm$^2$ . The initial height decreases by 1.91% from 1.51 to 1.49 mm. The frozen height decreases by 1.91% from 2.09 to 2.05 mm. Compared with the effect of inclined angle, the effect of droplet volume is greater.

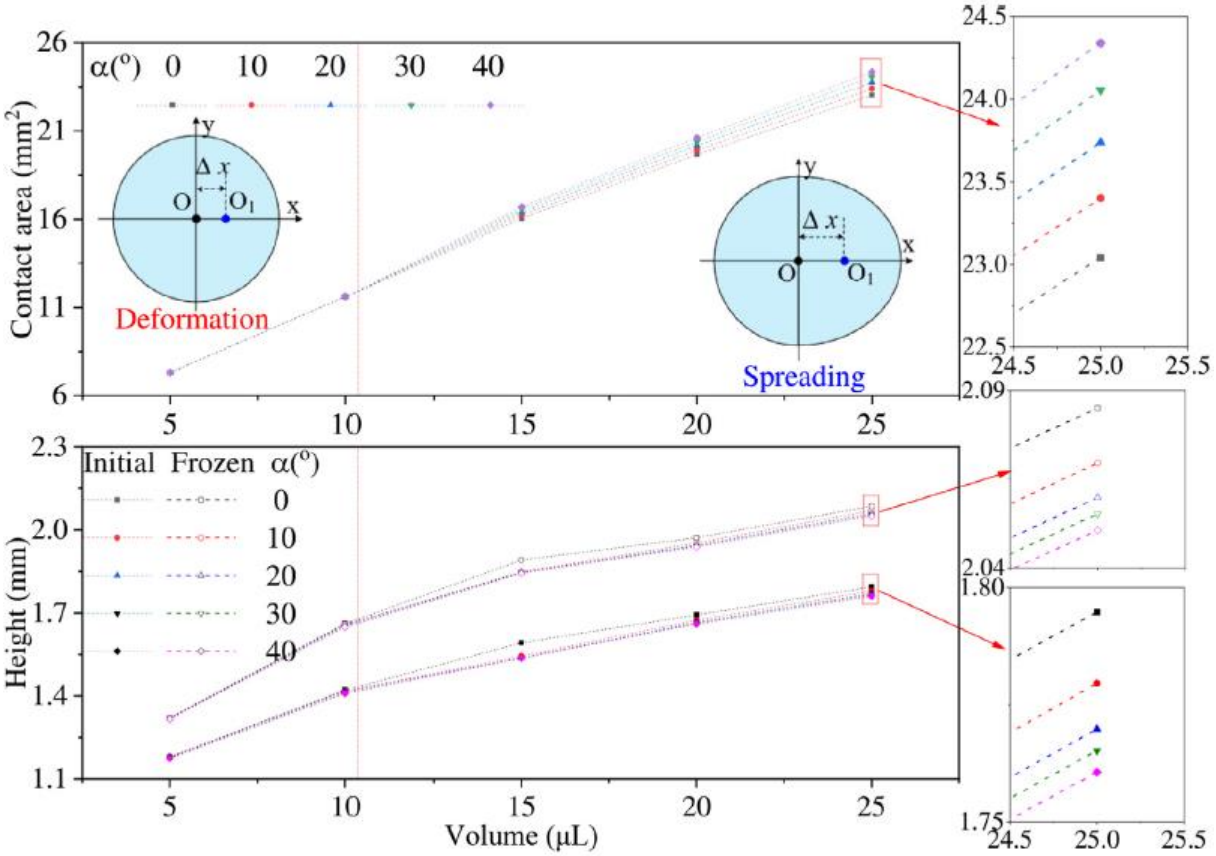


**Fig. 11**. Calculated variations contact area and height with volume and inclined angle.

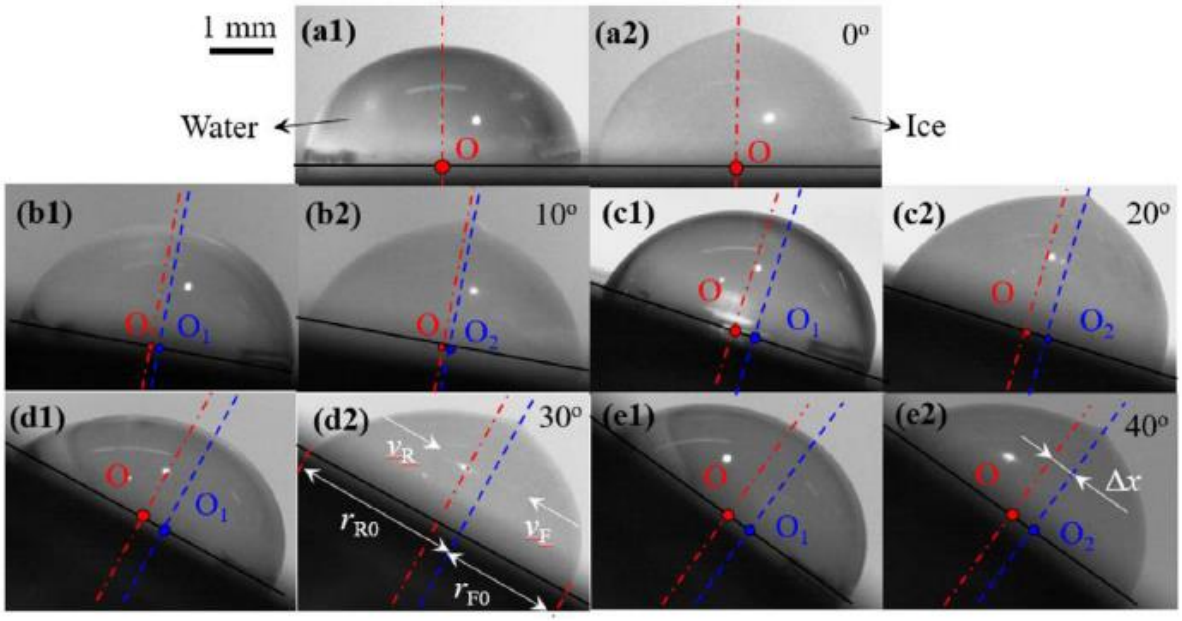


**Fig. 12**. Comparison of vertex offset between 20 $\mu$L initial and frozen profiles.

When the droplet volume increases from 5 to 25 $\mu$L on 40° inclined surface, the contact area increases by 232.84% from 7.31 to 24.34 mm$^2$ . The initial and frozen heights increase by 49.95% from 1.76 mm to 1.17 mm, and by 55.70% from 1.32 mm to 2.05 mm, respectively. According to calculated results, the effect of inclined angle on droplet under spreading type is greater than that under deformation type. And the effect of droplet volume on freezing process is greater than that of inclined angle.

To investigate the vertex offsets of initial and frozen droplets on cold plate surface, the comparisons of vertex offsets between 20 $\mu$L initial and frozen profiles on inclined surfaces are shown in **Fig. 12**. For a 20 $\mu$L water droplet on horizontal surface, the vertex subpoints of initial and frozen droplets on inclined surface are both at red point $O$, as shown in **Fig. 12**(a1) and (a2). When surface is titled, the gravity center of droplet would shift due to gravity effect and the vertex also shift. The vertex subpoint of initial droplet would change from red point O to blue point $O_1$, as shown in **Fig. 12**(b1). The initial rear radius $r_{R0}$ is larger than initial front radius $r_{F0}$ . Before rear and front angles decrease to the critical angle, the horizontal freezing rate at rear side $v_R$ is larger than that at front side $v_F$. When rear and front angles decrease to critical angle, $v_R$ is equal to vF until end. The subpoints of frozen tip on inclined surface is $O_2$. The phenomenon that the location of $O_1$ is the same as that of $O_2$, as shown in **Fig. 12**(b1-e1) and (b2-e2). For water droplets of which volumes are less than 25 $\mu$L and surfaces with inclined angles of 0 ~ 40°, the vertex subpoints of droplet on inclined surface are nearly not changed during freezing process.

Because frozen tip has a larger contact area with air. Frozen tips are more prone to frosting, compared with other locations of frozen water droplet. It is necessary to study the location of the frozen tip formation. Variation of vertex offset with droplet volume and inclined angle calculated by model are shown in **Fig. 13**. Compared with inclined angle, the volume effect on vertex offset is greater, which means the gravity effect on droplet shape is greater than that of inclined angle. For example, when a 10 qL droplet is placed on a surface of which inclined angle increases from 0° to 50°, the vertex offset increases by 9.85 mm. But when the inclined angle is 50° and the droplet volume increases from 10 to 12.5 $\mu$L, the vertex offset increases by 17.27 mm. On same inclined surface, vertex offset of water droplet under spreading type is larger than that of water droplet under deformation type. Volume

10.34 $\mu$L is the boundary line between deformation and spreading types, because the effect of surface tension on droplet profile is larger than that of gravity for water droplet under deformation type. The variation of vertex offset with inclined angle of surface for water droplet under deformation type is less than that for droplet under spreading type. When inclined angle increases from 10° to 50°, the vertex offsets for 5 $\mu$L water droplet increases by 57.02% from 3.63 x 10-2 mm to 5.70 x 10-2 mm, when that for 20 $\mu$L water droplet increases by 287.90% from 13.89 x 10-2 mm to 53.88 x 10-2 mm. These fundamental data may be used to control the location of frozen tip and thus control the frost layer on water droplet.

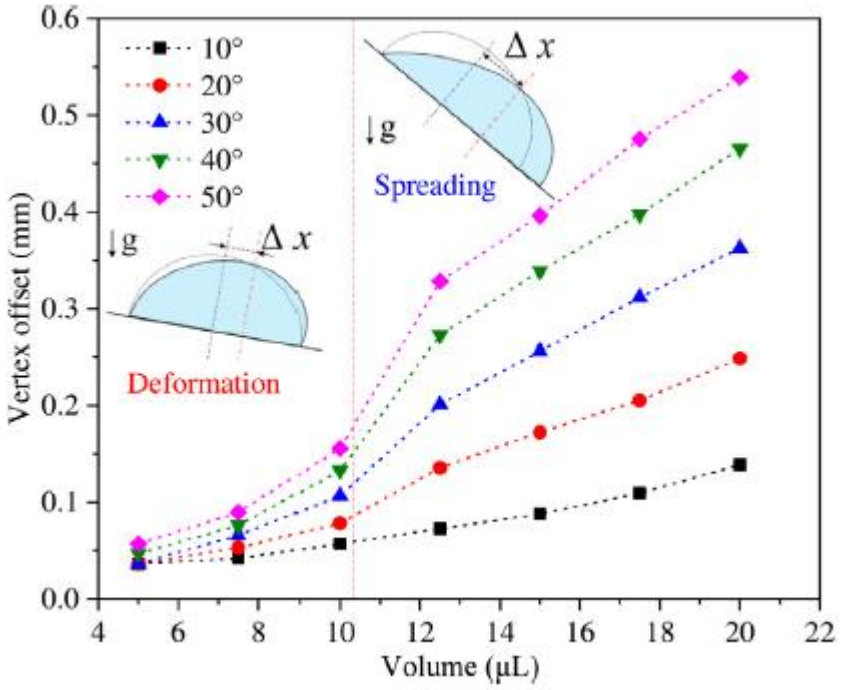


**Fig. 13**. Calculated evolutions of vertex offset with droplet volume and inclined angle.

The comparison of tip angles between experimental and calculated results is shown in **Fig. 14**. For experimental results, the tip angles are all in the range of 135° $\pm$ 5°. This also demonstrates that the size of frozen tip is independent with droplet volume and inclined angle of surface. For calculated results of model, the tip angles are in the range of 148° $\pm$ 5°. The deviation percentage between experimental and calculated results are about 9.63%. It is mainly caused by the reason that this model assumes that the gas concentration of water droplet is 0% and thus frozen water droplets do not contain trapped air bubbles. The density of ice without air bubbles is 916.70 kg/m$^3$. Actually, the water used in experiment contains gas. When the water droplet is frozen, the gas would be precipitated and trapped in droplet to form trapped bubbles. By calculation based on volume expansion ratio, the density of frozen water droplets used in the experiment is about 897 kg/m$^3$. The gas concentration is 1.70%. The tip angle of water droplet is influenced by gas concentration. When gas concentration of water droplet increases, the volume expansion after frozen increases and tip becomes shaper.

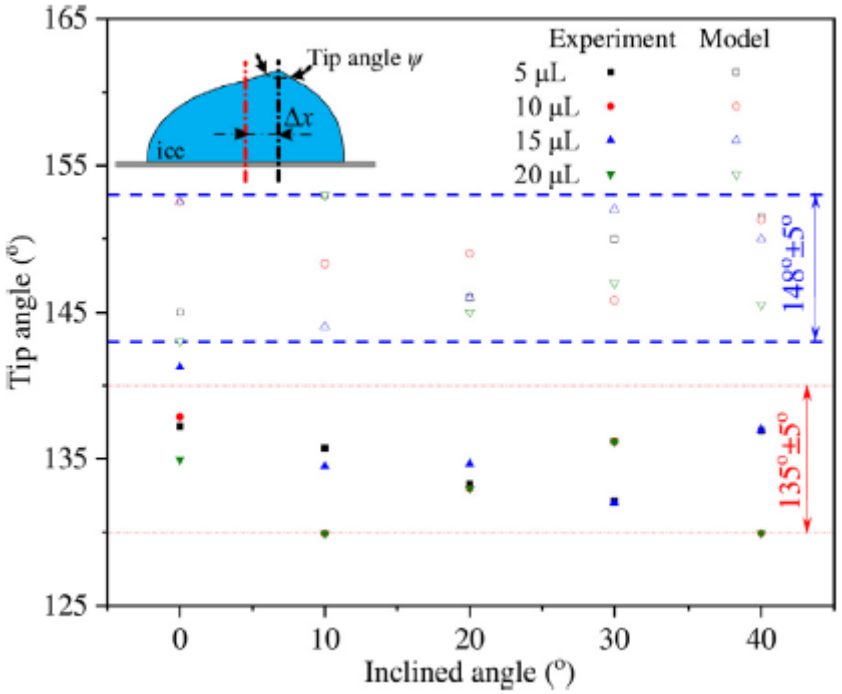


**Fig. 14**. Frozen tip angles of different droplets on different inclined surfaces.

As mentioned in our previous work [**39**], the formation of frozen tip is influenced by critical angle. The main factors of critical angle include initial droplet contact angle on horizontal surface and physical properties of the water droplet. For example, frozen tip of urine droplet is rounded [**39**]. Urine is less polarity than water due to the impurity like urea. The surface tension increases with the increase of liquid polarity. The surface tension of urine is less than that of water. Meanwhile, the density of urine is larger than that of water. Bond number of urine droplet is larger than that of water droplet. This means the critical angle of the former is less than of the latter, and thus the tip of former is blunter than that of latter, even rounded tip formation. The critical angles for water droplet with initial contact angle 78 ° and 125° are 14.4° and 25° [**40**], respectively. This also means that the critical angle increases with the increase of initial contact angle $\theta_0$.

**4.Discussion**

In this model, the heat conduction at the freezing front of droplet is assumed to be one-dimensional. In fact, this assumption can only be used during constant section heat conduction, such as freezing process of liquid column as shown in **Fig. 15**(a). The area of the freezing front is constant during freezing process of water column. But during freezing process of water droplet, the area of the freezing front decreases. As shown in **Fig. 15**(a) and (b), the bottom radii of water column and droplet are both $R_1$. When water column and droplet are frozen at the same height $H_1$ , the frozen volume of liquid column is V^ larger than that of droplet. And thus, the freezing process of water droplet is faster than that of liquid column. The freezing rate $v_1$ of column is larger than that of droplet $v_2$. Although deviation of calculated results would be caused by the assumption of one-dimensional heat conduction, the deviations of freezing rate are less than 6%, as shown in **Fig. 8**(b). Because only small-scale droplets of which volumes are less than 25 $\mu$L are studied by this model. Therefore, the assumption can be used in this model.

During calculation process, heat transfer and evaporation between droplet and air are negligible. In fact, due to temperature of surrounding air larger than that of water, the heat transfer between freezing water and air would occur and thus small amounts of unfrozen water would be evaporated. Because the area of droplet-gas interface and freezing duration increase as the increase of droplet volume. The amount of heat transfer between freezing water and air for big droplet is larger than that for small droplet, as shown in **Fig. 15**(b) and (c). The calculated deviation of heat transfer for big droplet is larger than that for small droplet under same condition. But freezing duration is short and the amount of heat transfer between water and air is much less than that between water and cold plate surface. For example, when 10.1 $\mu$L droplet was frozen on surface of -9 °C and gas temperature was 1 °C, the maximum heat transfer rate crossing the droplet-gas interface was 5.9 x 10-3 W, while that across the droplet-cold surface area was about 68 times larger at 4.0 x 10-1 W [**41**]. The ratio was also similar for 19.8 $\mu$L droplet under the same condition. In this study, experimental conditions are different. The gas temperature around droplet in acrylic chamber was kept at 6.3 °C. The cases of surface temperature are set in the range of -30 ∼-10 °C. The calculated heat transfer rate across droplet-cold plate is at least about 11.3 times greater than that across droplet-gas interface. Therefore, the assumption that heat transfer and evaporation between droplet and air are negligible can be adopted in this model.

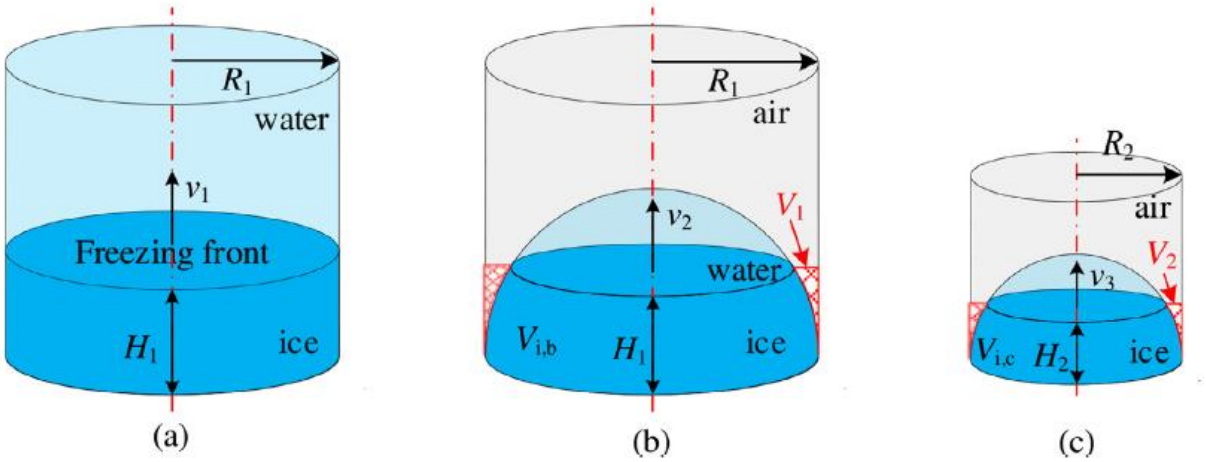


**Fig. 15**.ic diagram of freezing process of liquid column and droplet.

## 5. Conclusions

To further explore freezing characteristics of sessile water droplets on inclined surface, a theoretical model based on heat-enthalpy method is presented. The following conclusions could be summarized.

1) The dynamic behavior of droplets during surface tilting process could be divided into two types, deformation and spreading. A theoretical model is presented to simulate the freezing process of water droplet on inclined surface, with dynamic behavior considered. Average deviations of calculated profiles and freezing durations are both less than 5%, at 4.34% and 3.83%, respectively.
2) The effect of inclined angle on droplet of which volume is less than 10.34 $\mu$L is greater than that larger than 10.34 $\mu$L. When the inclined angle of surface changes from 0° to 40°, the contact area keeps at 11.61 mm$^2$ for 10 $\mu$L water droplet, and increases by 5.64% from 23.04 mm2 to 24.34 mm$^2$ for 25 qL water droplet, respectively. The frozen heights decrease by 0.76% and 1.91%, respectively.

3) Compared to the effect of inclined angle, the effect of droplet volume is greater. When the droplet volume increases from 5 to 25 $\mu$L on 40° inclined surface, the contact area increases by 232.84% from 7.31 to 24.34 $mm^2$. The initial and frozen heights increase by 49.95% from 1.76 mm to 1.17 mm, and by 55.70% from 1.32 mm to 2.05 mm, respectively.
4) Vertex offsets of water droplets of which volume are less than 10.34 $\mu$L are greater than that larger than 10.34 $\mu$L. When inclined angle of surface increases from 10° to 50°, the vertex offset increases by 57.02% from 3.63 x $10^{-2}$ mm to 5.70 x $10^{-2}$ mm for 5 $\mu$L water droplet, and by 287.90% from 13.89 x $10^{-2}$ mm to 53.88 x $10^{-2}$ mm for 20 $\mu$L water droplet.
5) Critical angle is the main condition of conical frozen tip formation, because the balance between the effects of gravity and surface tension on unfrozen droplet shape is broken when front and rear angles decrease to critical angle. For water droplet with gas concentration of 1.70%, its critical angle is all in the range of 15° $\pm$ 5° and its frozen tip angle is in the range of 135° $\pm$ 5°.

**References**


[1] M.J. Song, S.W. Lei, S.H. Hosseini, X.Y. Luo, Z.H. Wang, An experimental study on the effect of horizontal cold plate surface temperature on frosting characteristics under natural convection, Appl. Therm. Eng. 211 (2022) 118416.

[2] S.W. Lei, M.J. Song, C.B. Dang, Y.J. Xu, K.K. Shao, Experimental study on the effect of surface temperature on the frost characteristics of an inverted cold plate under natural convection, Appl. Therm. Eng. 211 (2022) 118470.

[3] L. Zhang, M.J. Song, S.M. Deng, J. Shen, C.B. Dang, Frosting mechanism and behaviors on surfaces with simple geometries: a state-of-the-art literature review, Appl. Therm. Eng. 215 (2022) 118984.

[4] H.Y. Deng, S.N. Chang, M.J. Song, The optimization of simulated icing environment by adjusting the arrangement of nozzles in an atomization equipment for the anti-icing and deicing of aircrafts, Int. J. Heat Mass Transf. 155 (2020) 119720.

[5] W.L. Lian, Y.M. Xuan, Experimental investigation on a novel aero-engine nose cone anti-icing system, Appl. Therm. Eng. 121 (2017) 1011-1021.

[6] S.W. Lei, M.J. Song, S.M. Deng, J. Shen, C.B. Dang, Experimental study on the effect of surface temperature on the frost characteristics of a vertical cold plate under natural convection, Exp. Therm. Fluid Sci. 215 (2022) 118984.

[7] J. Koszut, K. Boyina, G. Popovic, J. Carpenter, S. Wang, N. Miljkovic, Superhydrophobic heat exchangers delay frost formation and reduce defrost energy input of aircraft environmental control systems, Int. J. Heat Mass Transf. 189 (2022) 122669.

[8] S.W. Lei, M.J. Song, P. Libor, J. Shen, A numerical study on frosting and its early stage under forced convection conditions with surface and environmental factors considered, Sustain. Energy Technol. Assess. 45 (2021) 101202 .

[9] G. Chaudhary, R. Li, Freezing of water droplets on solid surfaces: an experimental and numerical study, Exp. Therm. Fluid Sci. 57 (2014) 86-93.

[10] M.H. Kim, D.R. Kim, K.S. Lee, Stochastic approach to the anti-freezing behaviors of superhydrophobic surfaces, Int. J. Heat Mass Transf. 106 (2017) 841-846.

[11] S. Sastry, Water: ins and outs of ice nucleation, Nature 438 (2005) 746-747.

[12] O.R. Enríquez, Á.G. Marín, K.G. Winkels, J.H. Snoeijer, Freezing singularities in water drops, Phys. Fluids 24 (2012) 091102.

[13] J.H. Snoeijer, P. Brunet, Pointy ice-drops: how water freezes into a singular shape, Am. J. Phys. 80 (2012) 764-771.

[14] X. Zhang, X. Liu, X.M. Wu, J.C. Min, Experimental investigation and statistical analysis of icing nucleation characteristics of sessile water droplets, Exp. Therm. Fluid Sci. 99 (2018) 26-34.

[15] A.G. Marin, O.R. Enriquez, P. Brunet, P. Colinet, J.H. Snoeijer, Universality of tip singularity formation in freezing water drops, Phys. Rev. Lett. 113 (5) (2014) 54301.

[16] Y.L. Li, M.X. Li, C.B. Dang, X.T. Liu, Effects of dissolved gas on the nucleation and growth of ice crystals in freezing droplets, Int. J. Heat Mass Transf. 184 (2022) 122334.

[17] Z.Y. Jin, Z.N. Wang, D.Y. Sui, Z.G. Yang, The impact and freezing processes of a water droplet on different inclined cold surfaces, Int. J. Heat Mass Transf. 97 (2016) 211-223.

[18] C.E. Clavijo, J. Crockett, D. Maynes, Hydrodynamics of droplet impingement on hot surfaces of varying wettability, Int. J. Heat Mass Transf. 108 (2017) 1717-1726.

[19] F.Q. Zhu, W.Z. Fang, T.H. New, Y.G. Zhao, C. Yang, Freezing morphologies of impact water droplets on an inclined subcooled surface, Int. J. Heat Mass Transf. 181 (2021) 121843.

[20] Z.Y. Jin, H.H. Zhang, Z.G. Yang, The impact and freezing processes of a water droplet on a cold surface with different inclined angles, Int. J. Heat Mass Transf. 103 (2016) 886-893.

[21] M.F. Ismail, P.R. Waghmare, Universality in freezing of an asymmetric drop, Appl. Phys. Lett. 109 (2016) 234105.

[22] A. Starostin, V. Strelnikov, L.A. Dombrovsky, S. Shoval, O. Gendelman, E. Bormashenko, Effect of asymmetric cooling of sessile droplets on orientation of the freezing tip, J. Colloid Interface Sci. 620 (2022) 179-186.

[23] X. Zhang, X.M. Wu, J.C. Min, X. Liu, Modelling of sessile water droplet shape evolution during freezing with consideration of supercooling effect, Appl. Therm. Eng. 125 (2017) 644-651.

[24] X. Zhao, B. Dorng, W.Z. Li, B.L. Dou, An improved enthalpy-based lattice Boltzmann model for heat and mass transfer of the freezing process, Appl. Therm. Eng. 111 (2017) 1477-1486.

[25] T.V. Vu, A.V. Truong, N.T.B. Hoang, D.K. Tran, Numerical investigations of solidification around a circular cylinder under forced convection, J. Mech. Sci. Technol. 30 (2016) 5019-5028.

[26] M.L. Lu, M.J. Song, Z.J. Ma, X.T. Wang, L. Zhang, A modeling study of sessile water droplet on the cold plate surface during freezing under natural convection with gravity effect considered, Int. J. Multiph. Flow 143 (2021) 103749.

[27] J.J. Sun, J.Y. Gong, G.J. Li, A lattice Boltzmann model for solidification of water droplet on cold flat plate, Int. J. Refrig. 59 (2015) 53-64.

[28] T.V. Vu, C.T. Nguyen, Q.H. Luu, Numerical study of a liquid drop on an inclined surface with solidification, Int. J. Heat Mass Transf. 144 (2019) 118636.

[29] M.L. Lu, M.J. Song, X.L. Pang, C.B. Dang, L. Zhang, Modeling study on sessile water droplet during freezing with the consideration of gravity, supercooling, and volume expansion effects, Int. J. Multiph. Flow 147 (2022) 103909 .

[30] T.V. Vu, G. Tryggvason, S. Homma, J.C. Wells, Numerical investigations of drop solidification on a cold plate in the presence of volume change, Int. J. Multiph. Flow 76 (2015) 73-85.

[31] J.D. Coninck, J.C. Fernández-Toledano, F. Dunlop, T. Huillet, A. Sodji, Shape of pendent droplets under a tilted surface, Phys. D 415 (2021) 132765.

[32] T. Young, An essay on the cohesion of fluids, Philos. Trans. R. Soc. 95 (1805) 65-87.

[33] A.W. Adamson, A. P. Gast, Physical Chemistry of Surfaces, 6th ed., Wiley, New York, 1997 .

[34] A. I. ElSherbini, A. M. Jacobi, Liquid drops on vertical and inclined surfaces I. An experimental study of drop geometry, J. Colloid Interface Sci. 273 (2 0 04)556-565.

[35] A. Rathinasamy, D. Ahmadian, P. Nair, Second-order balanced stochastic Runge-Kutta methods with multi-dimensional studies, J. Comput. Appl. Math. 377 (2020) 112890.

[36] I.K. Argyros, J. Ceballosb, D. González, J.M. Gutiérrez, Extending the applicability of Newton's method for a class of boundary value problems using the shooting method, Appl. Math. Comput. 384 (2020) 125378.

[37] H. Lomas, Calculation of front and rear contact angles: I. drops on inclined planes, J. Colloid Interface Sci. 33 (4) (1970) 548-553.

[38] Y.H. Jiang, W. Xu, M.A. Sarshar, C.H. Choi, Generalized models for front and rear contact angles of fakir droplets on pillared and pored surfaces, J. Colloid Interface Sci. 552 (15) (2019) 359-371 .

[39] Q. Dang, M.J. Song, C.B. Dang, T.Z. Zhan, L. Zhang, Experimental study on solidification characteristics of sessile urine droplets on a horizontal cold plate surface under natural convection, Langmuir 38 (25) (2022) 7846-7857.

[40] X. Zhang, X. Liu, J.C. Min, X.M. Wu, Shape variation and unique tip formation of a sessile water droplet during freezing, Appl. Therm. Eng. 147 (2019) 927-934.

[41] J.E. Castillo, Y. Huang, Z. Pan, J.A. Weibel, Quantifying the pathways of latent heat dissipation during droplet freezing on cooled substrates, Int. J. Heat Mass Transf. 164 (2021) 120608.